High-biomass sorghum yield estimate with aerial imagery

Ruixiu Sui,[a] Brandon E. Hartley,[b] John M. Gibson,[b] Chenghai Yang,[c] J. Alex Thomasson,[b] and Stephen W. Searcy[b]

[a] USDA-ARS Crop Production Research Unit, P. O. Box 350, Stoneville, Mississippi 38776
ruixiu.sui@ars.usda.gov

[b] Texas A&M University, Biological and Agricultural Engineering Department, College Station, Texas 77843

[c] USDA-ARS Kika de la Garza Subtropical Agricultural Research Center, Weslaco, Texas 78596

Abstract. To reach the goals laid out by the U.S. Government for displacing fossil fuels with biofuels, high-biomass sorghum is well-suited to achieving this goal because it requires less water per unit dry biomass and can produce very high biomass yields. In order to make biofuels economically competitive with fossil fuels it is essential to maximize production efficiency throughout the system. The goal of this study was to use remote sensing technologies to optimize the yield and harvest logistics of high-biomass sorghum with respect to production costs based on spatial variability within and among fields. Specific objectives were to compare yield to aerial multispectral imagery and develop predictive relationships. A 19.2-ha high-biomass sorghum field was selected as a study site and aerial multispectral images were acquired with a four-camera imaging system on July 17, 2009. Sorghum plant samples were collected at predetermined geographic coordinates to determine biomass yield. Aerial images were processed to find relationships between image reflectance and yield of the biomass sorghum. Results showed that sorghum biomass yield in early August was closely related ($R^2 = 0.76$) to spectral reflectance. However, in the late season the correlations between the biomass yield and spectral reflectance were not as positive as in the early season. The eventual outcome of this work could lead to predicted-yield maps based on remotely sensed images, which could be used in developing field management practices to optimize yield and harvest logistics. [DOI: 10.1117/1.3586795]

Keywords: biomass logistics; remote sensing; sorghum; yield; biofuels.

Paper 11056R received Apr. 6, 2011; revised manuscript received Apr. 12, 2011; accepted for publication Apr. 13, 2011; published online May 9, 2011.

1 Introduction

Agricultural production of dedicated biomass crops is a required part of the objective of displacing fossil fuels with renewable energy. Relative to other crops, sorghum is an excellent choice for dedicated biomass production because it requires less water per unit dry biomass and can produce very high biomass yields. There remains a great need for technologies that will enable production of high-biomass sorghum at as low a cost as possible. Without these technologies, history dictates that this energy source will not be competitive with other energy sources.

One of the problems is that energy density in biomass is low relative to fossil fuels, so large production savings are essential. This economic obstacle may be overcome by optimizing yield and harvest logistics with respect to production costs based partly on spatial variability within and among fields. One optimization technique that has proven viable in commercial

1931-3195/2011/$25.00 © 2011 SPIE

crop production is remote sensing (RS), which enables a large volume of data about a crop to be gained inexpensively over a large area. RS has been used in crop production to develop application maps for crop inputs, the use of which has in some cases reduced the amount of chemicals applied and the expense associated with them.

Some broad-scale predictive studies of RS relative to bioenergy have been conducted to assess land-cover type and biomass density concerning the utilization of forests as a biomass source. However, it is important to look at field studies in which a dedicated feedstock is produced. We must know whether a crop that produces a large amount of biomass can be produced inexpensively enough to make it worthwhile as an energy source. Minimizing costs at every link in the supply chain is critical, and RS is a tool for optimizing the yield-to-input ratio on a spatially variable basis.

The use of RS in agriculture is based on relationships between crop biophysical phenomena and their spectral signatures. RS has been used in water management, yield prediction, nutrient management, and pest management in a number of crops.[1] In sorghum, spectral and thermal-infrared data have been used to accurately model grain yield, and generalized relationships across multiple years and locations have been developed.[2,3] RS water stress indices have been found useful in optimizing irrigation strategies for sorghum.[4] Satellite imagery has been used to accurately estimate leaf area index in sorghum.[5] Microwave RS has been used to estimate sorghum chlorophyll content, which was highly correlated with the occurrence of pests.[6] RS and yield monitor data have been used to map sorghum plant growth and yield variability, indicating that RS could be used to correct problems in these areas.[7]

Spectral reflectances from image data have often been used to calculate vegetation indices. Normalized difference vegetation index (NDVI) is one of the vegetation indices that have been commonly used in remote-sensing applications in agriculture.[8–12] Other vegetation indices including reflectance band ratios and individual band reflectance have also been employed for crop management and yield prediction.[7,12–15]

The literature has clearly shown that RS is promising for many aspects of sorghum production management such as yield prediction, irrigation scheduling, and pest management. Earlier studies on the relationships between the plant canopy spectral and thermal features and physiological characteristics have provided solid fundamentals upon which further research can build. However, using RS in high-biomass sorghum presents several challenges. While traditional sorghum production is concerned with maximizing grain yield, the goal with high-biomass sorghum is maximizing total biomass. Thus, procedures in the literature that relate plant spectral features and various stress indices to grain yields will require re-examination and refinement. For farmers who might plant high-biomass sorghum, this study can give them tools for timely and site-specific evaluation of the health status of their crop and prescriptions for variable-rate applications of crop inputs that could greatly reduce their input costs. Furthermore, the ability to predict the biomass yield within a field or a group of fields can provide great advantages in terms of scheduling fleets of harvesting machinery, transport vehicles, and storage facilities. This issue is a very costly part of the production process, and its importance should not be underestimated.

The overall goal of this research was to use RS in developing high-biomass sorghum production methods that are as low-cost as possible in terms of crop inputs, and harvest and transport expenses. The specific objective of the study reported in this article was to estimate yield of high-biomass sorghum with aerial multispectral RS imagery.

2 Materials and Methods

2.1 Study Site

A 19.2-ha sorghum field (96.431685°W, 30.530911°N), located at the Texas AgriLife Research Farm in Burleson County, Texas, was selected as a research site. Two varieties of sorghum were planted on May 7, 2009. Ceres ES 5150, identified as a Sudan sorghum, was planted on 9.1 ha,

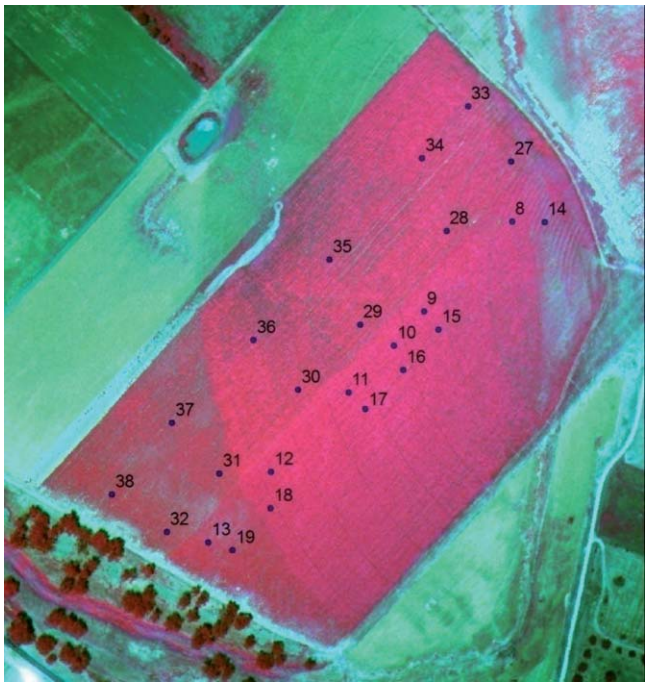

Fig. 1 Sampling location IDs superimposed on a color-infrared image of the high-biomass sorghum field.

and Ceres ES 5200, identified as an energy sorghum, was planted on 10.1 ha. The predominant soil type in the field is Belk clay (BaA), 0% to 1% slope, rarely flooded. The following are two other significant soil types in the field: Weswood silty clay (WwA) loam, 0% to 1% slope, rarely flooded, and Yahola fine sandy loam (YaB), 0% to 2% slope, rarely flooded. About five-sixths of the field was irrigated by a central pivot irrigation system and the rest was rain-fed. The field was further split into two different row spacings, 0.19 and 0.57 m.

A soil-EC map of the field was used to identify areas of different soil characteristics. Sampling points were chosen to obtain adequate field representation based on variations in soil electrical conductivity (EC) and irrigation, and biomass yield and quality variability were the primary output considerations. Twenty-four points within the field were chosen as initial sampling locations; point IDs were 8 to 19 and 27 to 38 (Fig. 1). Properties at each location are given in Table 1.

2.2 Harvesting and Sampling

A related research project was conducted at the same time with the objectives of determining optimal harvest time and developing appropriate logistic strategies for sorghum biomass handling. Sorghum biomass was harvested multiple times from late July 2009 to January 2010. Four of these harvests, from late July to early November, 2009, were included in this research. The area harvested during each of the four harvests included 6 of the 24 sampling locations. The first harvest (1.98 ha, sampling locations 14 to 19) was conducted from July 29 to August 6 (referred to as early August). The second harvest (1.98 ha, sampling locations 8 to 13) was conducted from August 20 to August 27 (late August). The third harvest (4.17 ha, locations 27 to 32) was conducted from October 20 to October 30 (late October), and the last harvest (1.25 ha, sampling locations 33 to 38) was conducted from November 6 to November 10 (early November). In terms of variety, the variety ES 5150 was harvested in early August and late August, and ES 5200 was harvested in late October and early November.

Table 1 Properties of initial sampling locations.

Location ID	Water	Soil type	Row spacing (m)	Variety	Harvest
8	Irrigated	WwA & BaA	0.57	ES 5150	late August
9	Irrigated	BaA	0.57	ES 5150	late August
10	Irrigated	BaA	0.57	ES 5150	late August
11	Irrigated	BaA	0.19	ES 5150	late August
12	Irrigated	BaA	0.19	ES 5150	late August
13	Rain-fed	BaA	0.19	ES 5150	late August
14	Irrigated	YaB & WwA	0.57	ES 5150	early August
15	Irrigated	BaA	0.57	ES 5150	early August
16	Irrigated	BaA	0.57	ES 5150	early August
17	Irrigated	BaA	0.19	ES 5150	early August
18	Irrigated	BaA	0.19	ES 5150	early August
19	Rain-fed	BaA	0.19	ES 5150	early August
27	Irrigated	BaA & WwA	0.57	ES 5200	late October
28	Irrigated	BaA	0.57	ES 5200	late October
29	Irrigated	BaA	0.57	ES 5200	late October
30	Irrigated	BaA	0.19	ES 5200	late October
31	Rain-fed	BaA	0.19	ES 5200	late October
32	Rain-fed	BaA	0.19	ES 5200	late October
33	Irrigated	BaA	0.57	ES 5200	early November
34	Irrigated	BaA	0.57	ES 5200	early November
35	Irrigated	BaA	0.57	ES 5200	early November
36	Irrigated	BaA	0.19	ES 5200	early November
37	Rain-fed	BaA	0.19	ES 5200	early November
38	Rain-fed	BaA	0.19	ES 5200	early November

In the first three harvests, four types of machine conditioners were used for conditioning sorghum stover: Macdon SP Windrower with 16′ R80 Rotary Disc header (referred to as MD), Macdon SP Windrower with 16′ A40 auger sickle cutter-bar header (referred to as MA), John Deere SP Windrower with 14.5′ rotary disc header and impeller conditioner, and John Deere Windrower with 14.5′ rotary disc header and tri-lobe steel conditioner. In the last harvest only two types of conditioner (MD and MA) were used instead of four. Soon after conditioning, sorghum biomass yield samples were taken at points around each sampling location for each conditioner. Therefore, 24 samples (6 locations, 4 types of conditioners) were taken on a daily basis for each of the first 3 harvests, and 12 samples (6 locations, 2 types of conditioners) for the last harvest. On a few occasions time constraints prevented all 24 samples from being taken during the first three harvests. For each conditioner type and sampling location, seven yield samples were collected in the first harvest, six collected in the second, three in the third, and two in the fourth, except for those few occasions where time was limiting.

For each conditioner type, a handheld global positioning system (GPS) receiver was used to identify sample points around the initial sampling locations. Then the surrounding area was observed to establish a representative portion of the windrow. Once this "average area" was located, a wooden frame was placed over the sample area, giving an outline of the full windrow width and 0.67 m length for cutting. After cutting around the windrow frame with an edger, the sorghum was placed into a bag and weighed before being transported back to the lab. The sample was ground at the lab with a chipper shredder. Subsamples were randomly collected from the shredder collection bag until an adequate amount of biomass was retrieved, and each subsample was frozen at -19°C for future moisture content determination. All samples were later dried at 105°C until there was no measureable change in sample weight.

2.3 Image Acquisition and Processing

A high resolution, four-camera, aerial imaging system described by Yang[16] was used for image acquisition in this study. A multispectral image of the sorghum field was acquired with the system on July 14, 2009, 68 days after planting. The system acquired 12-bit images with

Table 2 Correlations between sorghum biomass yield in early August and reflectance spectra of sorghum plant canopy using multiple linear regression ($n = 24$).

Independent variables[a]	R^2	Pr > F
RVI	0.710	<0.0001
NDVI	0.679	<0.0001
Red	0.586	<0.0001
NIR	0.580	<0.0001
Blue	0.317	0.0042
Green	0.136	0.0761
NDVI RVI	0.720	<0.0001
Red NDVI	0.692	<0.0001
NIR Red NDVI	0.722	<0.0001
NIR Red Blue NDVI	0.746	<0.0001
NIR Red Blue NDVI RVI	0.757	<0.0001
NIR Red Green Blue NDVI RVI	0.757	0.0002

[a]Dependent variable is sorghum biomass yield in early August, 2009.

2048 × 2048 pixels in blue (430 to 470 nm), green (530 to 570 nm), red (630 to 670 nm), and near-infrared (NIR) (810 to 850 nm) wavelength intervals. The multispectral image was acquired at an altitude of 2590 m, and pixel size was approximately 1 m. The image was geo-referenced to the UTM coordinate system with a set of GPS reference points on the ground.

Digital count values of the blue, green, red and NIR bands were extracted with a 3-pixel × 3-pixel window centered at each of the sampling points. The values from the nine pixels for each point were averaged for each band. The procedures for image rectification and data extraction were performed with ERDAS IMAGINE software (Leica Geosystems Geospatial Imaging, LLC, Norcross, Georgia). The vegetation indices, NDVI and RVI (ratio vegetation index), were computed for each sampling point. NDVI was calculated by dividing the difference between the NIR and red digital count values by the sum of NIR and red count values; i.e., NDVI = (NIR − red)/(NIR + red). RVI was the band ratio of the NIR to red; i.e., RVI = NIR/red.

Yield of sorghum biomass at each sampling point was estimated with the dry weight of the sample and the sampling area (3.066 m^2). Yield estimates of each harvest were averaged by the sampling point for each type of machine conditioner, giving 84 yield estimates including 24 in the early August harvest (6 sampling locations × 4 types of machine conditioners), 24 in late August (6 locations × 4 types of machine), 24 in late Oct (6 locations × 4 types of machine), and 12 in early November (6 locations × 2 types of machine).

Vegetation indices (NDVI and RVI) and digital count values of each individual band (NIR, blue, green, and red) were analyzed with multiple linear regression (SAS software, PROC REG procedure; SAS Institute Inc., Cary, North Carolina) to determine the relationships between the sorghum biomass yield and the indices and the digital count values. An analysis of variance (ANOVA) test was also conducted to determine the effect of row spacing on NDVI.

3 Results and Discussion

Analyses were conducted to determine relationships between sorghum biomass yield and NDVI, RVI and digital count values at blue, green, red, and NIR bands at each of the four harvests. Results are given in Tables 2–5. Overall, the early August yield had the best relationship ($R^2 = 0.757$) with RS data. For variety, ES 5150, RVI and NDVI were well correlated with yield ($R^2 = 0.710$ and 0.679), and the NIR and red bands were more sensitive to yield than the blue and green bands: this was expected from the literature. The model having the highest correlation coefficient for each variety was selected to be used in estimating yield. Yield estimates were plotted against actual yield (Fig. 2). Models for ES 5150 at the early August and late August harvests performed better in predicting the yield ($R^2 = 0.757$ and 0.647, respectively) than those for ES 5200 at the October and November harvest ($R^2 = 0.450$ and 0.517, respectively).

Table 3 Correlations between sorghum biomass yield in late August and reflectance spectra of sorghum plant canopy using multiple linear regression ($n = 24$).

Independent variables[a]	R^2	Pr > F
RVI	0.414	0.0007
NDVI	0.444	0.0004
Red	0.306	0.0051
NIR	0.479	0.0002
Blue	0.030	0.4162
Green	0.145	0.0668
NIR blue	0.511	0.0005
NIR blue NDVI	0.574	0.0006
NIR green blue NDVI	0.590	0.0014
NIR green blue NDVI RVI	0.647	0.0012
NIR green blue red NDVI RVI	0.647	0.0033
Green blue NDVI RVI	0.639	0.0004
Green blue NDVI	0.589	0.0004
Blue NDVI	0.570	0.0001

[a]Dependent variable is sorghum biomass yield in late August, 2009.

Table 4 Correlations between sorghum biomass yield in late October and reflectance spectra of sorghum plant canopy using multiple linear regression ($n = 24$).

Independent variables[a]	R^2	Pr > F
RVI	0.016	0.5530
NDVI	0.014	0.5796
Red	0.080	0.1793
NIR	0.011	0.6213
Blue	0.064	0.2330
Green	0.004	0.7765
Red green	0.129	0.2350
NIR red green	0.347	0.0333
NIR red green RVI	0.387	0.0449
NIR red green Blue RVI	0.435	0.0500
NIR green blue red NDVI RVI	0.450	0.0809
Red green blue NDVI RVI	0.450	0.0411
Red green NDVI RVI	0.393	0.0414
Red green NDVI	0.345	0.0340

[a]Dependent variable is sorghum biomass yield in late October, 2009.

Table 5 Correlations between sorghum biomass yield in early November and reflectance spectra of sorghum plant canopy using multiple linear regression ($n = 12$).

Independent variables[a]	R^2	Pr > F
RVI	0.273	0.0813
NDVI	0.247	0.1001
Red	0.136	0.2374
NIR	0.270	0.0834
Blue	0.027	0.6080
Green	0.036	0.5566
NDVI RVI	0.404	0.0978
NIR red green Blue NDVI RVI	0.517	0.5610
NIR red green NDVI RVI	0.516	0.3817
NIR red green NDVI	0.513	0.2257
NIR red NDVI	0.483	0.1339
NIR red	0.283	0.2236

[a]Dependent variable is sorghum biomass yield in early November, 2009.

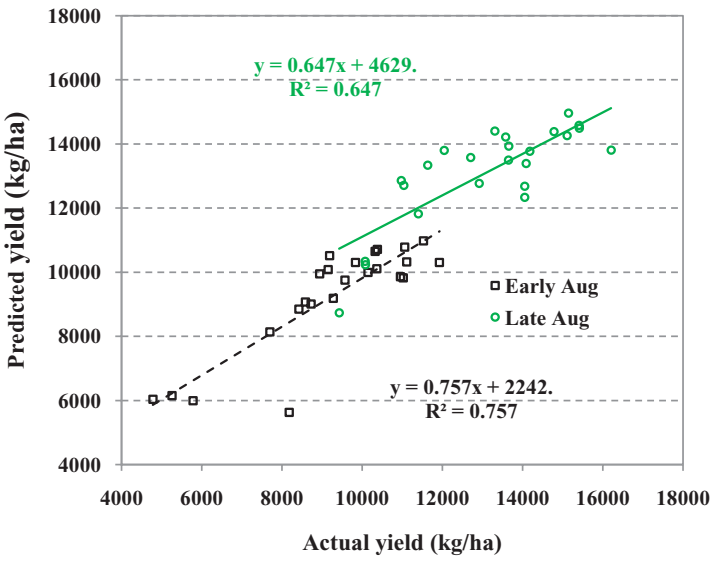

Fig. 2 Actual sorghum biomass yield versus the predicted yield for early and late August sampling dates.

The poorer relationship between models and biomass of ES 5200 could have been caused by harvesting date or variety or both. Figure 3 indicates that ES 5150 accumulated biomass after the early August harvest. Average yield was 9258 dry kg/ha at early August and increased 42%, up to 13121 dry kg/ha, by late August. The date (July 14th) when the image was acquired was closer to the date of the early August harvest, so the image was likely a better reflection of growth status at this harvest. The ES 5200 variety was harvested in late October and early November and yield exhibited no obvious differences between these two harvests (18,811 and 18,376 dry kg/ ha). The lesser (2.3%) yield in early November could be due to degradation of the biomass in field.

NDVI distribution across the initial sampling locations is shown in Fig. 4. Except for location 14, which has a different soil type (WwA & BaA), the ES 5150 variety had a higher NDVI value

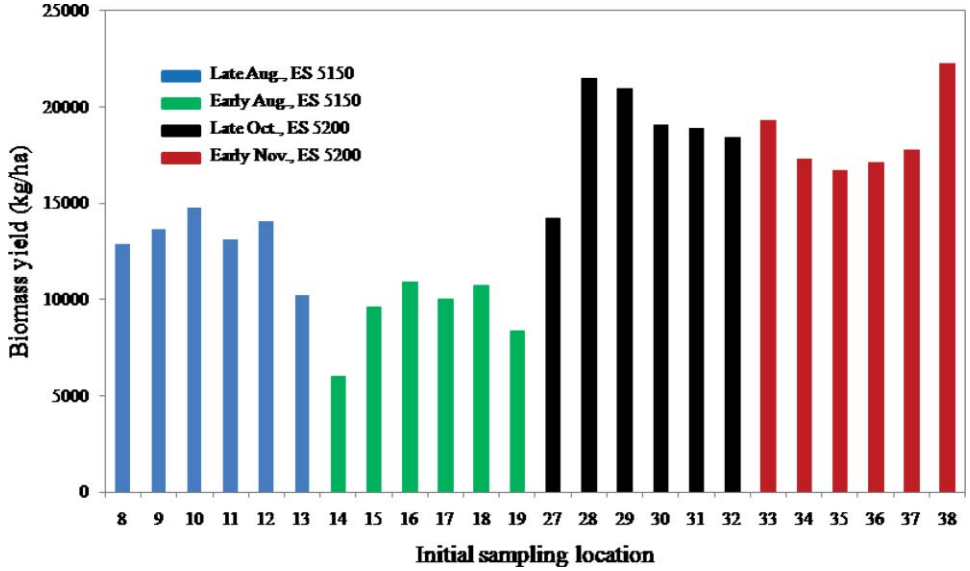

Fig. 3 Yield of sorghum dry biomass at initial sampling locations.

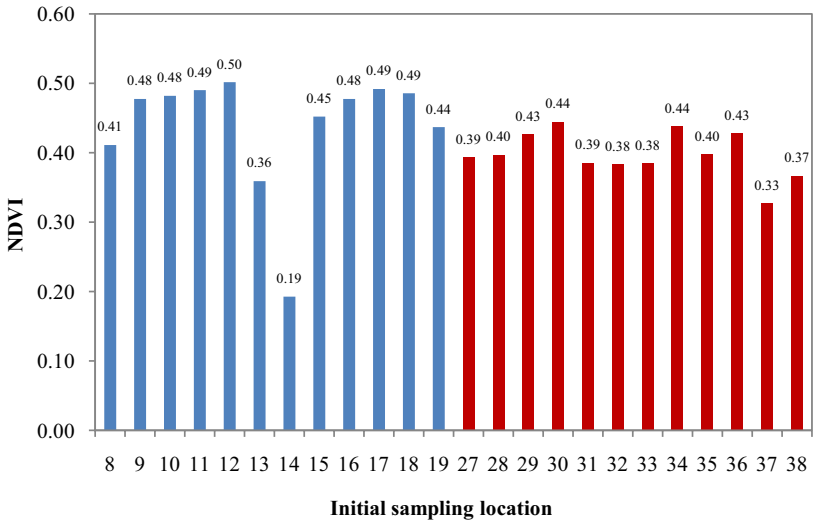

Fig. 4 NDVI values of sorghum variety ES 5150 (location 8 to 14) and ES 5200 (location 27 to 38) on July 14, 2009.

than ES 5200. This difference likely relates to the fact that the ES 5150 had a better developed plant canopy than ES 5200. In general, full canopy coverage benefits the assessment of plant growth conditions with RS imagery.

Spectral reflectance from the plant canopy may have been affected by irrigation conditions and row spacing as well. The average NDVI value (Fig. 4) was 0.42 for ES 5150 and 0.40 for ES 5200. NDVI values in all rain-fed locations except location 19 were lower than the variety average; thus, irrigation generally increased NDVI. Results of the ANOVA test dealing with the effect of row spacing on NDVI indicated no significant difference in NDVI between areas with 0.57 m spacing and those with 0.19 m spacing [$F(1, 82) = 1.72, p = 0.1937$].

Other factors that could affect accuracy of the models in predicting sorghum biomass yield relate to the biomass samples used to calculate the yield. One factor relates to how yield samples were collected, and the other relates to the large amount of variability in moisture content. It was noted during biomass harvesting that slug feeding occurred at times with the conditioning machines. This situation was generally caused by a build-up of biomass in front of the machine and a subsequent lack of flow followed by a larger than normal flow of biomass into a windrow. The uneven flow through the conditioners caused unevenness in the windrows, both along the row and across the row, in height of the windrow and density of the material within the windrow. Selecting a representative sample of the windrow under these circumstances is difficult and prone to error. It was also observed that after rainfall events, water tended to collect near the bottom of the windrow. There were thus significant inconsistencies in moisture content throughout the windrow, particularly when samples were taken soon after a rainfall event. Therefore, it was again difficult to select a representative sample from the windrow, and the process was more prone to error after a rainfall event.

4 Summary and Conclusion

Biomass sorghum yield was found to be well correlated with aerial multispectral imagery. Two varieties of biomass sorghum grown in a 19.2-ha field with different growth conditions were selected for the study. The biomass sorghum was harvested and biomass yield samples were collected at 84 sampling points. Multispectral imagery of the sorghum field was acquired during the growing season in four wavebands (NIR, red, green, and blue) with an aerial remote sensing system. Relationships between sorghum biomass yield and spectral reflectance were analyzed, and yield was closely related to the reflectance parameters ($R^2 = 0.757$) and could be estimated

fairly well even with a model only involving the band ratio of NIR to red ($R^2 = 0.710$) during the early August harvest. At the late August harvest, multiple regression analysis also indicated a good correlation between the yield and the spectral reflectance ($R^2 = 0.647$). Results of this study point to the potential of using aerial multispectral imagery to estimate biomass sorghum yield. However, to obtain a more accurate yield prediction, issues such as image acquisition time, large variability of the biomass moisture content, and biomass yield sampling should be properly addressed in the development of prediction models with remote sensing imagery data.

Mention of a commercial product is solely for the purpose of providing specific information and should not be construed as a product endorsement by the authors or the institutions with which the authors are affiliated.

References

1. P. J. Pinter, J. H. Hatfield, J. S. Schepers, E. M. Barnes, M. S. Moran, C. S. T. Daughtry, and D. R. Upchurch, "Remote sensing for crop management," *Photogramm. Eng. Remote Sens.* **69**(6), 647–664 (2003).
2. J. L. Hatfield, "Remote-sensing estimators of potential and actual crop yield," *Remote Sens. Environ.* **13**(4), 301–311 (1983).
3. A. J. Richardson, C. L. Wiegand, D. F. Wanjura, D. Dusek, and J. L. Steiner, "Multisite analyses of spectral-biophysical data for sorghum," *Remote Sens. Environ.* **41**, 71–82 (1992).
4. A. E. Ajayi, and A. A. Olufayo, "Evaluation of two temperature stress indices to estimate grain sorghum yield and evapotranspiration," *Agron. J.* **96**, 1282–1287 (2004).
5. S. J. Maas, "Using satellite data to improve model estimates of crop yield," *Agron. J.* **80**, 655–662 (1988).
6. D. Singh, R. Sao, and K. P. Singh, "A remote sensing assessment of pest infestation on sorghum," *Adv. Space Res.* **39**, 155–163 (2007).
7. C. Yang, J. H. Everitt, J. M. Bradford, and D. E. Escobar, "Mapping grain sorghum growth and yield variations using airborne multispectral digital imagery," *Trans. ASAE* **43**(6), 1927–1938 (2000).
8. S. G. Bajwa, and L. F. Tian, "Aerial CIR remote sensing for weed density mapping in a soybean field," *Trans. ASAE* **6**, 1965–1974 (2001).
9. R. E. Plant, D. S. Munk, B. R. Roberts, R. L. Vargas, D. W. Rains, R. L. Travis, and R. B. Hutmacher, "Relationships between remotely sensed reflectance data and cotton growth and yield," *Trans. ASAE* **43**(3), 535–546 (2000).
10. H. Sembiring, W. R. Raun, G. V. Johnson, M. L. Stone, J. B. Solie, and S. B. Phillips, "Detection of nitrogen and phosphorus nutrient status in winter wheat using spectral radiance," *J. Plant Nutrition* **21**(6), 1207–1232 (1998).
11. C. L. Wiegand, A. J. Richardson, D. E. Escobar, and A. H. Gerbermann, "Vegetation indices in crop assessments," *Remote Sens. Environ.* **35**, 105–119 (1991).
12. C. Yang, and J. H. Everitt, "Relationships between yield monitor data and airborne multidate multispectral digital imagery for grain sorghum," *Precision Agriculture* **3**(4), 373–388 (2002).
13. A. Dobermann, and J. L. Ping, "Geostatistical integration of yield monitor data and remote sensing improves yield maps," *Agron. J.* **96**, 285–297 (2004).
14. D. M. El-Shikha, E. M. Barnes, T. R. Clarke, D. J. Hunsaker, J. A. Haberland, P. J. Pinter, Jr., P. M. Waller, and T. L. Thompson, "Remote sensing of cotton nitrogen status using the canopy chlorophyll content index (CCCI)," *Trans. ASABE* **51**(1), 73–82 (2008).
15. R. Sui, J. B. Wilkerson, W. E. Hart, L. R. Wilhelm, and D. D. Howard, "Multi-spectral sensor for detection of nitrogen status in cotton," *Appl. Eng. Agric.* **21**(2), 167–172 (2005).
16. C. Yang, "An airborne four-camera imaging system for agricultural applications," ASABE Paper No. 10–08855, ASABE, St. Joseph, Michigan (2010).

Biographies and photographs of the authors not available.